Colocalization of Glial Fibrillary Acidic Protein, Metallothionein, and MHC II in Human, Rat, NOD/SCID, and Nude Mouse Skin Keratinocytes and Fibroblasts

Lusine Danielyan[1], Genrich Tolstonog[2], Peter Traub[2], Juergen Salvetter[3], Christoph H. Gleiter[1], Dieter Reisig[3], Rolf Gebhardt[4] and Gayane H. Buniatian[1,4]

The expression of glial fibrillary acidic protein (GFAP) by perivascular cells of many mammalian organs suggests an as yet unknown function of this intermediate filament protein in the maintenance of homeostasis and vascular permeability at the blood–tissue interface. Although a similar situation may exist at the air–tissue interface, the cellular distribution of GFAP in skin tissue has never been demonstrated. To approach this issue, we have employed immunofluorescence and Western blotting techniques to detect GFAP in skin sections of young and adult humans, normal rodents, and two types of mutant mice, as well as in rat lung sections, and in cultured human keratinocytes and fibroblasts. Colocalization with antigens known to be associated with GFAP in other tissues was also tested. Epidermal and hair follicle keratinocytes and dermal fibroblasts showed distinct staining for GFAP as well as colocalization with alpha-actin, metallothionein, and antigens of the class-II major histocompatibility complex (MHC II). GFAP was also identified in rat alveolar fibroblasts which, in common with keratinocytes, form part of the air–tissue interface. GFAP was upregulated together with MHC II in nude mice but was barely detectable in the skin of non-obese diabetic severe combined immunodeficiency mice, suggesting a possible involvement in antigen-presenting functions. The intriguing distribution of a common set of antigens both in certain cells of the integumentary system and at the blood–tissue interfaces of internal organs suggests the involvement of these proteins in universal mechanisms controlling tissue homeostasis and protection.

Journal of Investigative Dermatology (2007) **127,** 555–563. doi:10.1038/sj.jid.5700575; published online 28 September 2006

INTRODUCTION

Glial fibrillary acidic protein (GFAP) is a highly conserved intermediate filament (IF) protein originally considered as a marker protein for astrocytes (Brenner, 1994). Meanwhile, GFAP mRNA protein has also been detected in many non-neural cells of the same anatomy as astrocytes. An increasing body of evidence now demonstrates the accumulation of GFAP in lens epithelial cells, Leydig cells of testis, hepatic stellate cells (HSCs), podocytes, mesangial cells, pancreatic stellate cells, fibroblasts, and chondrocytes of elastic cartilage in epiglottis (for review, see Apte *et al.*, 1998; Buniatian, 2001; Hainfellner *et al.*, 2001). The common antigenic composition of GFAP-producing cells (GFAP-PCs) was interpreted as a hint on a possible similar developmental origin of these cells (Schulze *et al.*, 1987; Holash *et al.*, 1993; Cassiman *et al.*, 1999). In these cells, GFAP has been found to be associated with other IF proteins such as vimentin, desmin, nestin, and smooth muscle alpha-actin (SMAA; Lecain *et al.*, 1991; Bunn *et al.*, 1999; Buniatian *et al.*, 1999a, b; Steinert *et al.*, 1999; Lonigro *et al.*, 2001; Schwab *et al.*, 2001; Peterson *et al.*, 2004; Mani *et al.*, 2005). Even more surprising, in peripheral organs, GFAP-PCs, that is, HSC, kidney glomeruli mesangial cells, and podocytes were found to express certain proteins usually associated with brain-specific protecting functions of astrocytes such as metallothionein (MT) and major histocompatability complex II (MHC II) (Buniatian *et al.*, 2001; Lu *et al.*, 2001; Riccalton-Banks *et al.*, 2003). These observations led to the hypothesis that GFAP-PCs play an indispensable, but still largely

[1]*Department of Clinical Pharmacology, University Hospital, Tuebingen, Germany;* [2]*Max-Planck-Institut für Zellbiologie, Rosenhof, Ladenburg, Germany;* [3]*Institute of Anatomy, University of Leipzig, Leipzig, Germany and* [4]*Institute of Biochemistry, Medical Faculty of University of Leipzig, Leipzig, Germany*

Correspondence: Dr Gayane H. Buniatian, Institute of Biochemistry, Medical Faculty of University of Leipzig, Johannisallee 30, Leipzig D-04103, Germany. E-mail: buniatian@web.de

Abbreviations: CLS, confocal laser scanning; DAPI, 4′,6 diamidino-2-phenylindole; GFAP, glial fibrillary acidic protein; GFAP-PC, glial fibrillary acidic protein-producing cell; HSC, hepatic stellate cell; MHC, major histocompatibility complex; MT, metallothionein; NOD, non-obese diabetic; PBS, phosphate-buffered saline; SCID, severe combined immunodeficiency; SMAA, smooth muscle alpha-actin

Received 14 March 2006; revised 17 July 2006; accepted 7 August 2006; published online 28 September 2006

unknown role at the blood–tissue interface of neural and non-neural organs with respect to tissue protection and maintenance of homeostasis (Buniatian, 2001; Buniatian *et al.*, 2002). The apparent universality of this concept prompted us to investigate whether it might apply also to tissues of the integumentary system, that is, to cells located at the air–body interface. Therefore, we investigated the localization of GFAP in skin samples of different species including normal and mutant strains of mice. The latter, nude mice and non-obese diabetic (NOD)/severe combined immunodeficiency (SCID) mice, provided novel insight into possible functional aspects of the colocalization with MHC II and other antigens studied.

RESULTS

Human skin sections

In situ staining of human epidermal keratinocytes. Labelling of young human skin slices with monoclonal antibodies (mAb) (Figure 1a) or polyclonal antibodies (pAb) directed against bovine GFAP (Figure 1b) showed the presence of this astrocyte marker protein in keratinocytes through all layers of the epidermis: stratum basalis (white arrows throughout Figure 1), stratum spinosum, stratum granulosum, and stratum corneum (blue arrows throughout Figure 1). The non-filamentous GFAP staining pattern perfectly delineated the crypt-like structure of the epidermis and separated it from dermis. The strongest expression of GFAP was observed in keratinocytes in stratum corneum and in stratum basalis (Figure 1a and b). Localization of GFAP predominated in peripheral parts but also occurred in nuclear region of the cells (Figure 1b, c, and f).

The micrographs of mono- (Figure 1d) and double-immunofluorescence (Figure 1c) studies illustrate that desmin (red), another type III IF protein, was weakly produced in GFAP-expressing (green) keratinocytes. Vimentin (red), the third type III IF protein investigated in this study, was also weakly formed in epidermal keratinocytes (blue arrow in Figure 1e). Although SMAA was generally weak in epidermal keratinocytes, some cells showed a prominent nuclear staining (red, Figure 1g) that occasionally appeared yellow in the micrographs (Figure 1f), indicating colocalization of SMAA (red), and GFAP (green) in the nuclear region of some keratinocytes. GFAP was expressed in sweat glands, vessels, and hair follicles (yellow arrowheads, white arrowheads, red arrowheads in Figure 1h, respectively).

MT was strongly expressed in epidermal keratinocytes (red, Figure 1i). In the cornified layer of epidermis (blue arrow in Figure 1i), the cells produced high amounts of both, GFAP (green) and MT (red), resulting in yellow structures in merged micrographs (Figure 1i). Although GFAP and MT seemed equally coexpressed throughout the epidermis, in some regions, especially in the papilla (red arrow in Figure 1i), keratinocytes expressed MT (red) more strongly than GFAP (green).

In adult human skin, the pattern of GFAP (green) localization was not changed (Figure 1j and k). It was well expressed in skin epidermis and parts of dermis (Figure 1k), and was colocalized primarily with MHC-II (red in Figure 1j) in epidermal keratinocytes.

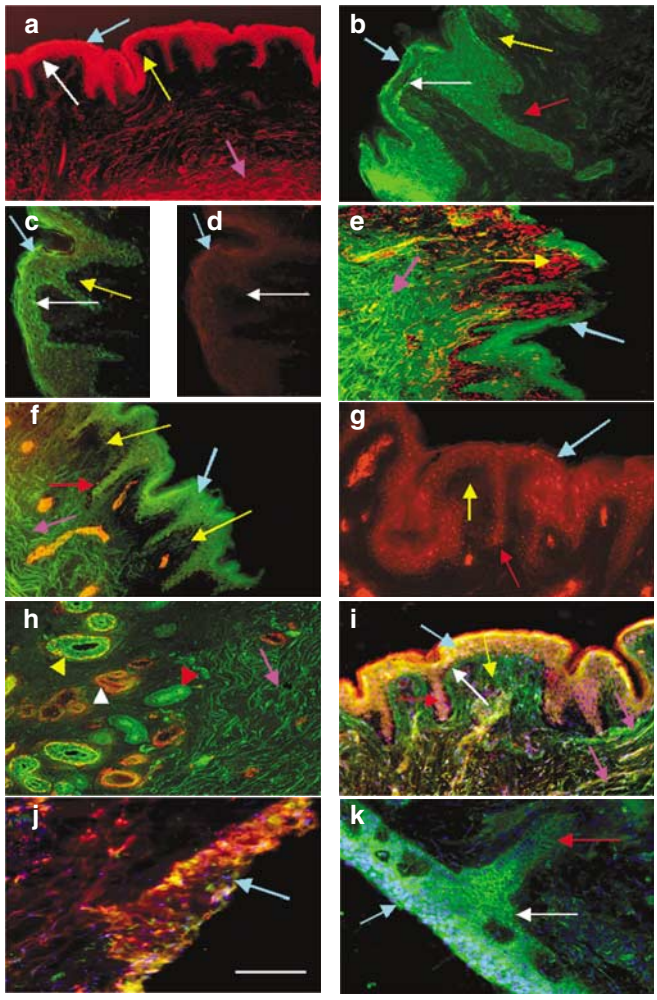

Figure 1. Astrocyte-associated antigens in (a–i) frozen young (10 years) and (j, k) adult human skin sections. (**a**) Expression of GFAP detected using mouse mAb GFAP. (**b**) Expression of GFAP detected using rabbit pAb GFAP. (**c**) Double staining for GFAP (green) and desmin (red). (**d**) Staining for desmin alone. (**e**) Double staining for GFAP (green) and vimentin (red). (**f**) Double staining for GFAP (green) and SMAA (red). (**g**) Staining for SMAA alone. (**h**) Double staining for GFAP (green) and SMAA (red). (**i**) Double staining for GFAP (green) and MT (red). (**j**) Double staining for GFAP (green) and MHC II (red). (**k**) Staining for GFAP (green). Blue arrows point to stratum corneum, white arrows to stratum basalis, yellow arrows to fibroblasts adjacent to stratum basalis, red arrows to papilla structures, and magenta arrows to fibroblasts in the lower layers of dermis. Yellow arrowheads to sweat glands, white arrowheads to vessels, and red arrowheads to hair follicles. Cy3-conjugated anti-mouse IgG from goat was used for the detection of mouse mAb GFAP, mAb desmin, mAb vimentin, mAb SMAA, and mAb MT-labelling sites. Skin structures labelled with rabbit pAb GFAP were detected using FITC-conjugated anti-rabbit IgG from goat. The preservation of skin structures and cells which could not be detected by distinct antibodies was ascertained by counterstaining of cell nuclei by DAPI (blue). Bar: in (**a**, **e**, **f**, **h**, **i**) = 10 μm; in (**b–d**, **g**, **j**, **k**) = 20 μm.

In situ staining of human dermal fibroblasts. Both, mAb GFAP (Figure 1a) and pAb GFAP (green in Figure 1b, c, e, f, h, and i), labelled some fibroblasts in the lower parts of the dermis (magenta arrows throughout Figure 1). In the upper

part of the dermis adjacent to the stratum basalis (yellow arrows throughout Figure 1), fibroblasts were barely detectable when labelled with antibodies against GFAP (green in Figure 1b, c, e, and f). Only in very few regions adjacent to the stratum basalis, fibroblastic cells labelled with pAb GFAP (yellow arrow in Figure 1i) could be observed. In contrast, mAb against vimentin (red) intensely labelled the fibroblasts adjacent to the stratum basalis of the epidermis (yellow arrow in Figure 1e).

In the lower dermis, most fibroblasts (magenta arrows in Figure 1) appeared to contain solely GFAP when simultaneously labelled with anti-GFAP (green) and anti-vimentin or anti-SMAA antibodies (red in Figure 1e and h, respectively). Only occasionally, GFAP was colocalized with vimentin (Figure 1e) or with SMAA (Figure 1f and h). However, GFAP and SMAA were colocalized in myofibroblastic cells forming the vascular walls of the capillaries and middle-sized vessels (white arrowheads in Figure 1h). GFAP-PCs could be observed also in the inner part of sweat glands (yellow arrowheads in Figure 1h) surrounded by a rim of contractile cells detected by SMAA staining (red). Furthermore, GFAP was expressed in keratinocytes surrounding the hair follicles (red arrows in Figure 1g). The intensity of MT staining (red in Figure 1i) in fibroblasts was weaker than that of GFAP (green in Figure 1i).

Cultured human skin cells

The presence of GFAP in human skin keratinocytes and fibroblasts was confirmed by immunocytochemical studies performed on cultured cells (Figure 2). The merged micrographs (Figure 2a) of double stainings for GFAP (green, Figure 2b) and MT (red, Figure 2c) of 14-day-old cultured human keratinocytes showed strong expression of MT in young small cobblestone-like cells, whereas GFAP was more intensely stained in large, flattened keratinocytes. Some cells produced equal amounts of GFAP and MT, as evidenced by bright, yellow staining in merged images, but there were also cells in which GFAP (green) prevailed over MT (red in Figure 2a). The heterogeneity in the intensity of staining for both proteins in neighboring cells was similar to that of seen by *in situ* staining (cf. Figure 2a with Figure 1i).

Nearly, equal reaction of GFAP (Figure 2e) and desmin (Figure 2f) in human fibroblasts from young cultures was evidenced by bright yellow staining in merged micrograph (Figure 2d) of these small cells. After 3 days in culture, fibroblasts were activated and rapidly proliferated (cf. Figure 2d and g). The differentiation of fibroblasts was accompanied by retraction of GFAP towards the perinuclear region and downregulation in peripheral parts of the cells (Figure 2h), increased expression of desmin (Figure 2i), and strong upregulation of SMAA (not shown).

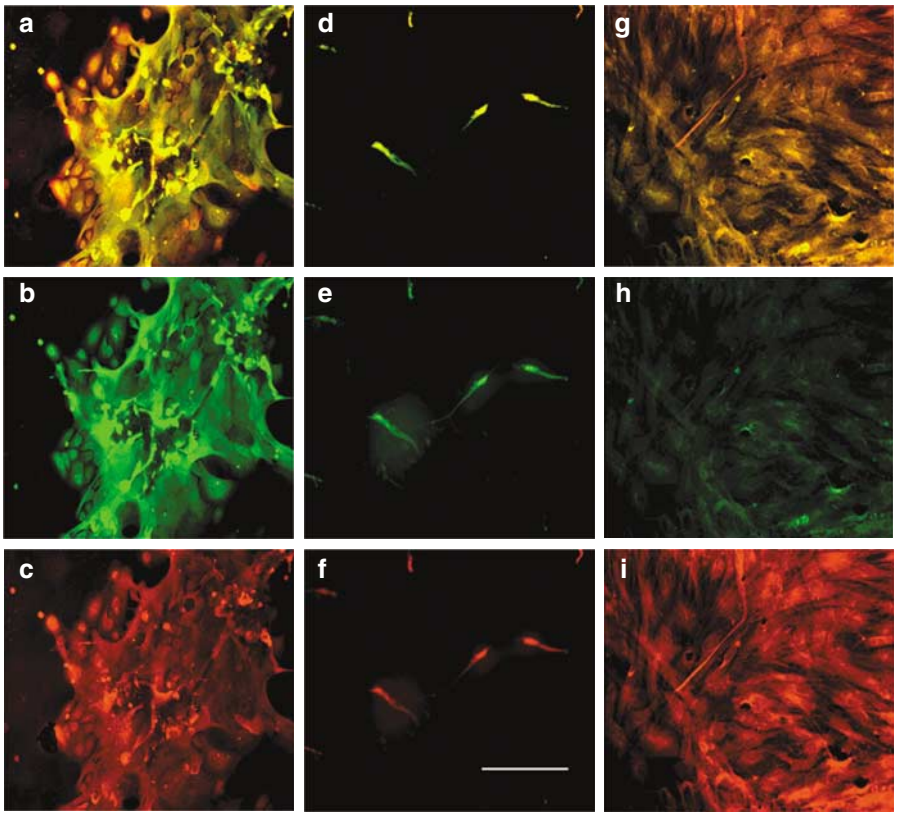

Figure 2. Differentiation of human keratinocytes and fibroblasts in culture. (**a–c**) Double labelling of 7-day-old keratinocytes with pAb GFAP and mAb MT: (**a**) merge of GFAP and MT staining; (**b**) staining for GFAP; and (**c**) staining for MT. (**d–f**) Double labelling of 2-day-old fibroblasts with pAb GFAP and mAb desmin: (**d**) merge of GFAP and desmin staining; (**e**) staining for GFAP; and (**f**) staining for desmin. (**g–i**) Double labelling of 7-day-old fibroblasts with pAb GFAP and mAb MT: (**g**) merge of GFAP and desmin staining; (**h**) staining for GFAP; and (**i**) staining for desmin. The secondary antibody used in (**b**, **e**, **h**) was rabbit antiserum FITC-conjugated anti-rabbit IgG from goat, whereas in (**c**, **f**, **i**) was Cy3-conjugated anti-mouse IgG from goat. Bar = 20 μm.

Rat skin sections

Epidermal keratinocytes from newborn rat skin (blue arrows throughout Figure 3) accumulated large amounts of GFAP (Figure 3a) and MHC II (Figure 3d), while weakly expressing SMAA (Figure 3b) and vimentin (not shown). MT was produced mainly by keratinocytes located in the inner layer of the epidermis, that is, stratum basalis (not shown). GFAP-expressing keratinocytes also delineated the outer sheet of hair follicles (magenta arrows in Figure 3c, e, and f). Concerning dermal fibroblasts, some of them solely expressed GFAP (yellow arrows pointing to green stained cells in Figure 3c, e, and f), vimentin (yellow arrows pointing to red stained cells in Figure 3f), or desmin (yellow arrows pointing to red stained cells in Figure 3e), whereas others coexpressed GFAP and vimentin, or desmin (different nuances of staining of the cells labelled with yellow arrows in the merged Figure 3c, e, and f). Inside hair follicles, GFAP, SMAA, MHC II were strongly expressed in the cuticle (Cu) and the medulla (M) of the hair channel (red arrows labelled with M throughout Figure 3). In the follicle cortex (white arrows throughout Figure 3), a population of cells surrounding the hair channel could be distinguished by 4′,6 diamidino-2-phenylindole (DAPI) staining (blue in Figure 3f) that did not stain for GFAP. In some follicles, however, the cortical cells weakly expressed GFAP (green in Figure 3a and e), and MHC II (red, Figure 3d).

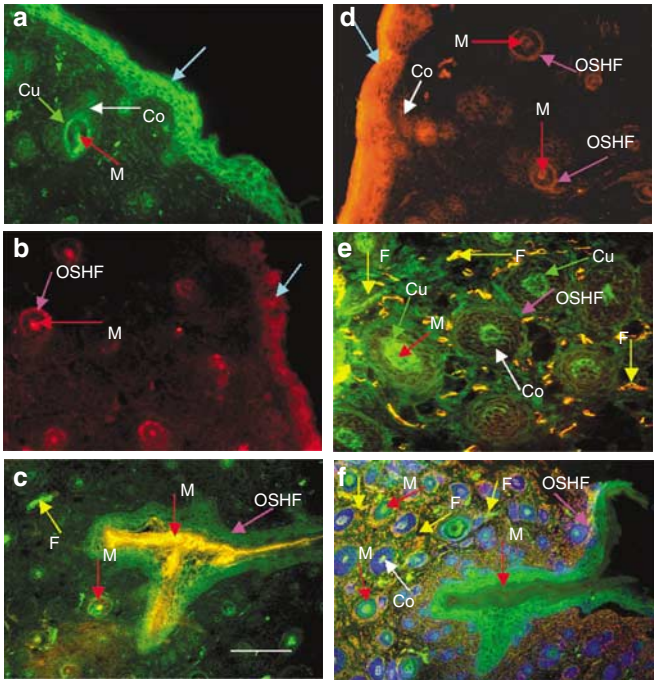

Figure 3. Astrocyte-associated antigens in frozen rat skin sections. (**a**) Labelling with pAb GFAP. (**b**) Labelling with mAb SMAA (red). (**c**) Double labelling with pAb GFAP (green) and mAb SMAA (red). (**d**) Labelling with mAb MHC II. (**e**) Double labelling with pAb GFAP (green) and mAb desmin (red). (**f**) Double labelling with pAb GFAP (green) and mAb vimentin. Skin structures labelled with anti-GFAP were detected using FITC-conjugated anti-rabbit IgG from goat, whereas Cy3-conjugated anti-mouse IgG from goat was used for detection of mAb desmin, mAb vimentin, mAb SMAA, and mAb MHC II. Blue arrows point to epidermis; yellow arrows to fibroblasts (F); white arrows to follicle cortex (Co); red arrows to cuticle (Cu); and magenta arrows to outer sheet of the hair follicles. Bar: in (**a–d**, **f**) = 10 μm; in (**e**) = 20 μm.

Mouse skin sections

GFAP was strongly expressed in the epidermis and dermis of CD1 BalbC (Figure 4b) and C57BL/6 mice (Figure 4e) similar to human and rat skin. However, both CD1 BalbC (Figure 4c) and C57BL/6 (Figure 4f) mouse strains overexpressed MHC II in dermis relative to the epidermis contrasting with the situation in humans and rats. In merged pictures (Figure 4a and d), colocalization of both antigens was evident, although the extent varied considerable ranging from slight costaining to bright yellow fields of cells particularly in dermis of CD1 BalbC mice (Figure 4a).

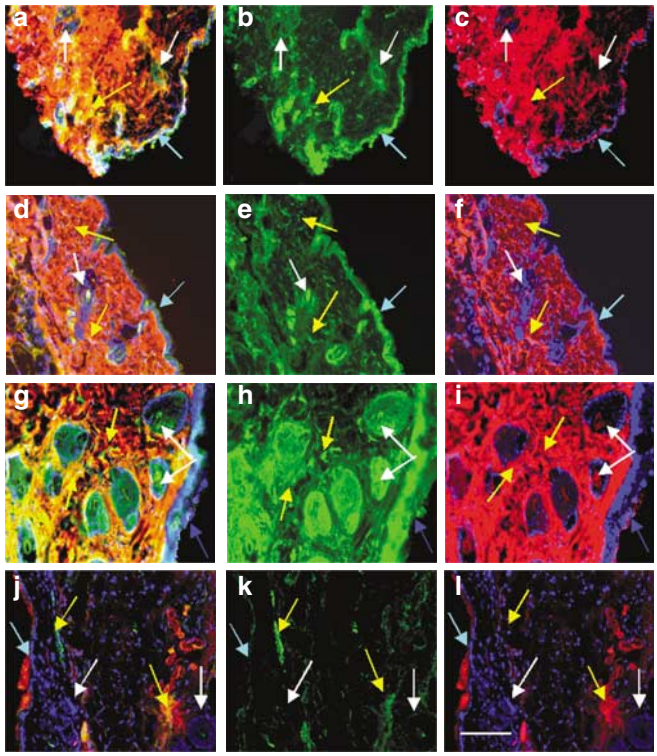

Figure 4. Colocalization of GFAP and MHC II in normal and mutant murine skin. (**a–c**) Double staining of CD1 Balb C mouse skin sections for GFAP and MHC. (**a**) Merged micrograph of GFAP and MHC immune reaction; (**b**) staining for GFAP; and (**c**) staining for MHC II. (**d–f**) Double staining of C75BL/6 mouse skin sections for GFAP and MHC II. (**d**) Merged micrograph of GFAP and MHC immune reaction; (**e**) staining for GFAP; and (**f**) staining for MHC II. (**g–i**) Double staining of CD1-Foxn1 nu nude mouse skin sections for GFAP and MHC. (**g**) Merged micrograph of GFAP and MHC immune reaction; (**h**) staining for GFAP; and (**i**) staining for MHC II. (**j–l**) Double staining of NOD-SCID mouse skin sections for GFAP and MHC. (**j**) Merged micrograph, staining for GFAP and MHC immune reaction; (**k**) staining for GFAP; and (**l**) staining for MHC II. Skin structures labelled with anti-GFAP were detected using FITC-conjugated anti-rabbit IgG from goat, whereas Cy3-conjugated anti-mouse IgG from goat was used for detection of mAb MHC II. Because MHC II was very strongly expressed in (**a**, **c**) CD1 BalbC, (**d**, **f**) C57BL/6, and in (**g**, **i**) nude mice, the images illustrating immunoreaction of MHC II had to be taken at 10-fold faster exposure (less sensitivity) than those of GFAP, whereas in (**j**, **l**) NOD/SCID mice exposure times were equal. Blue arrows point to epidermis; yellow arrows to dermal fibroblasts; and white arrows to follicles. Bar = 10 μm.

To test the hypothesis that GFAP might be associated with protection and antigen-presenting functions involving MHC II, we used two types of mutant mice, nude mice and NOD/SCID mice, which are *a priori* known to over- and under-express MHC II, respectively. In nude mice (Figure 4g–i), both MHC II (red) and GFAP (green) were upregulated. Careful inspection of the results of double-staining experiments showed that nearly all the cells stained for MHC also costained for GFAP (Figure 4g). This was evident by multiple yellow stained dermal cells in the merged micrograph in Figure 4g. In contrast to control BalbC and C57BL/6 mice skin in which cortical cells in the hair follicles were visualized only by DAPI and barely detectable staining for MHC II and GFAP, in nude mice the follicles were strongly enlarged and contained large amounts of GFAP (green, cf. white arrows in Figure 4b, e, and h). In the opening of these follicles, also few cells expressing MHC could be distinguished (Figure 4i).

In NOD/SCID mouse skin sections (Figure 4j–l), both GFAP (green, Figure 4k) and MHC II (red, Figure 4l) were strongly downregulated, both in dermis and epidermis. The skin of these mutant mice contained follicles which could be visualized only by nuclear staining with DAPI (white arrows in Figure 4j–l).

The authenticity of GFAP localization in skin

Different approaches were used to confirm the specificity of GFAP staining in different skin samples:

1. *Omission of primary antibodies*: In control immunolabelling studies performed on human (Figure 5e), rat, and mouse skin sections (not shown), the primary antibodies were omitted. The sections were treated only with a mixture of rabbit antiserum and FITC-conjugated anti-rabbit IgG from goat and Cy3-conjugated anti-mouse IgG from goat and mounted in mounting medium containing DAPI. This resulted in disappearance of the cellular contours – the cells could be identified only by bright DAPI-stained chromatin (Figure 5e).

2. *Confocal laser scanning (CLS) microscopy*: In Figure 5, representative serial optical sections are shown obtained by CLS microscopy of newborn rat skin slices (Figure 5a), cultured human skin fibroblasts (Figure 5c), as well as newborn rat lung slices (Figure 5d) immunolabelled with pAb GFAP. CLS immunofluorescence microscopy confirmed the results obtained by using widefield microscopy: GFAP is expressed in epidermal keratinocytes (blue arrows), in keratinocytes forming the outer sheet of hair follicles, in the hair cuticle (Cu), in the cortical area (Co) of the follicle (Figure 5a), and in dermal fibroblasts (Figure 5c). Moreover, CLS microscopy evidenced the presence of GFAP in the cytoplasm and nucleus of cultured skin fibroblasts (Figure 5c). To demonstrate that GFAP is also present in other cells contacting air, we performed a single experiment on newborn rat lung. CLS microscopy revealed the presence of GFAP in fibroblasts surrounding the alveoli (Figure 5d).

3. *Western blot assay*: The presence of GFAP in skin was confirmed also by Western blot assay (Figure 4f and g), demonstrating the specificity of mAb against GFAP. Immunoblot analysis was performed using protein extracts prepared from newborn rat skin (Figure 4f). The T6 cell line, an activated HSC line (Kim *et al.*, 1998), as well as extracts of 14-day-old astroglial cells were used for comparison (Figure 4g), that is, cells *a priori* known to contain GFAP. The immunoreaction with mAb GFAP uncovered two major bands with apparent molecular masses of ~55 and ~52 kDa in newborn rat skin. The thickness and intensity of staining of these bands diminished with decreasing protein concentration (Figure 4f). Similar patterns of immunoreaction were obtained in blots of the T6 cell line (Figure 4g, lane 1) and of astroglial cells (Figure 4g, lane 2). Weak immunoprecipitate in the samples

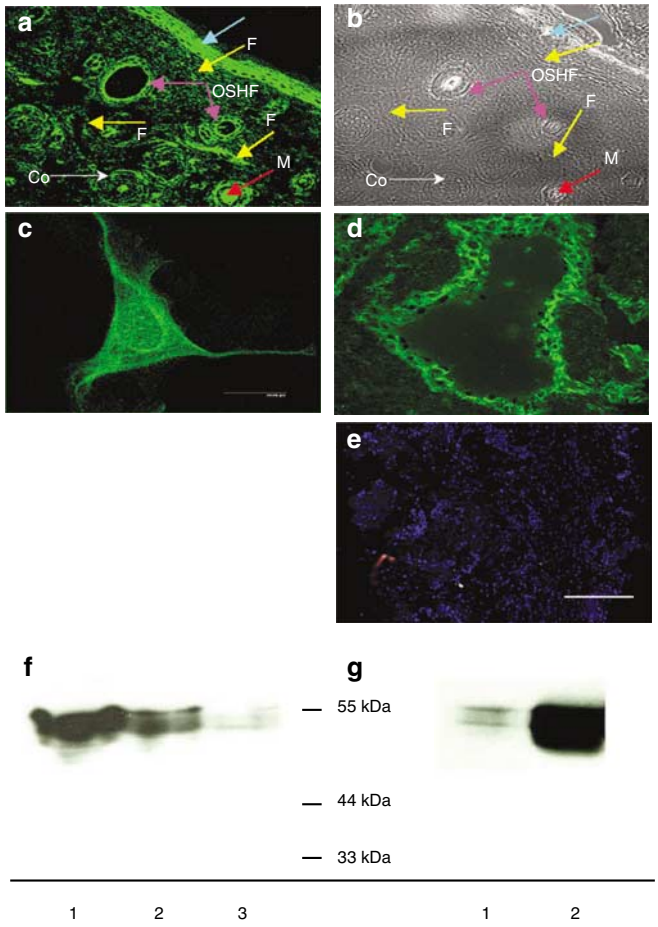

Figure 5. The authenticity of GFAP expression in skin. (**a–d**) CLS microscopy of skin preparations stained for GFAP. (**a**) Labelling of newborn rat skin sections with pAb GFAP. (**b**) Phase contrast micrograph of the field shown in (**a**). (**c**) Cultured human fibroblasts stained for GFAP. (**d**) Labelling of newborn rat lung section with pAb GFAP. GFAP was detected using rabbit antiserum and FITC-conjugated anti-rabbit IgG from goat. Blue arrows point to epidermis; yellow arrows to fibroblasts (f); white arrows to follicle cortex (Co); red arrows to cuticle (Cu); and magenta arrows to outer sheet of the hair follicles. (**e**) Control widefield immunofluorescence assay: human skin section treated with mixture of FITC-conjugated anti-rabbit IgG from goat and Cy3-conjugated anti-mouse IgG from goat. Bar: in (**a**, **b**) = 10 μm; in (**c**–**e**,) = 20 μm. (**f**, **g**) Immunoblot analysis of GFAP. (**f**) Immunoblot analysis of GFAP in homogenates of newborn rat skin (lane 1, 34.5 μg; lane 2, 3.0 μg; and lane 3, 1.5 μg); (**g**) immunoblot analysis of GFAP in homogenates of T6 cells (lane 1, 12.5 μg) and newborn rat astroglial culture (lane 2, 21.5 μg). In all tested tissues, mAb GFAP labelled two major protein bands with apparent molecular masses of ~55 and ~52 kDa.

of the T6 cell line (Figure 4g, lane 1) is in accordance with downregulation of GFAP during HSC activation (Buniatian *et al.*, 1996a; Niki *et al.*, 1996). Also, the abundance of GFAP in astroglial cells from confluent astroglial culture (Figure 4g, lane 2) is in accordance with the well-established capacity of differentiated astrocytes to produce large amounts of GFAP (Wagner *et al.*, 1993).

DISCUSSION

We describe here the presence of high levels of GFAP in the epidermis and dermis of both humans and rodents. This expression of GFAP at the air–tissue interface established by cells of the integumentary system parallels that previously described in both neural and non-neural cells adjacent to the blood–tissue interface.

The presence of GFAP in keratinocytes and skin fibroblasts was confirmed by both widefield and CLS microscopy using mAbs and pAbs, and by Western blot analysis. Our detection of GFAP in the nucleus of activated cultured fibroblasts is consistent with *in vitro* studies demonstrating the capacity of type III IF proteins to interact with DNA (Traub, 1995; Tolstonog *et al.*, 2000). As reported previously, selection of appropriate antibodies is essential for detecting GFAP in non-neural tissues (Hainfellner *et al.*, 2001). The consistent detection of a 55-kDa protein on Western blots strongly suggests that the mAb GFAP used here specifically recognizes GFAP. The additional 52-kDa band detected in the Western blots is likely to be a product of alternative splicing of rat GFAP mRNA as has been previously observed in rat brain, where four alternatively spliced transcripts have been detected (Condorelli *et al.*, 1999). Further evidence for the specificity of GFAP detection is provided by (a) heterogeneity in the pattern of GFAP staining between neighboring cells and regions of epidermis and dermis, (b) low overall staining intensity (with the exception of few areas in most of which GFAP was colocalized with MHC II) in skin sections of NOD/SCID mice which produce only small amounts of GFAP, and (c) absence of any staining in control sections treated with secondary antibodies only.

Our analyses have revealed a striking similarity between skin cells expressing GFAP and other GFAP-PCs at blood–tissue interfaces of internal organs with respect to the colocalization of certain antigens involved in protective functions, exemplified here by MHC II and MT. The skin raises an immune barrier to infection and possesses considerable innate immune capacity (Oren *et al.*, 2003; Dupasquier *et al.*, 2004). A number of studies have shown that keratinocytes are capable of initiating local immune responses by production of MHC II (Gaspari, 1997; Gaspari and Katz, 1988). Our results confirm these observations, but emphasize species-specific differences in this pattern. Whereas expression of MHC II in human and rat skin is higher in epidermis than in dermal fibroblasts, in both mouse strains it is higher in the dermis than in the epidermis. This may be explained by the recent finding of Dupasquier *et al.* (2004) that in normal murine species, macrophages and other CD45+ cells constitute a major subpopulation (about 70%) of cells in the dermis. The slight heterogeneity in the MHC II/GFAP ratio between different murine skin cells is consistent with previous observations of heterogeneity in the antigenic composition of antigen-presenting cells in murine dermis reported by Duraiswamy *et al.* (1994).

Most strikingly, our results point to a remarkable association between the antigen-presenting function of skin keratinocytes and fibroblasts and the expression of GFAP. This is most apparent in mutant mice of the nude phenotype (CD1 nu−/nu−), in which MHC II and GFAP are strongly upregulated in all dermal cells, although slight differences between different cell types may exist. GFAP upregulation is especially pronounced in the enlarged hair follicles characteristic for the nude phenotype and may be owing to a compensatory response to the downregulation of certain cytokeratins resulting from loss of the foxn1 transcription factor (for review, see Mecklenburg *et al.*, 2005). Whether the upregulation of MHC II is a direct or indirect consequence of the loss of foxn1 remains to be established. Interestingly, the hypertrophy of follicles in nude mice is a feature also observed during hair loss in humans. There, hypertrophy of follicles is known to be associated with a perifollicular lymphocytic infiltrate made up primarily of CD4+ cells, together with a CD8+ intrafollicular infiltrate and immune activation indicated by expression of HLA-DR; HLA-A, -B, and -C on the follicular epithelium (Gilhar and Kalish, 2006).

Conversely, in NOD/SCID mice, both GFAP and MHC II were barely detectable in the skin, either in the dermis or the epidermis. The NOD/SCID mice used here have a complex genotype, as they express only one MHC class II molecule: the I-A^{g7} allele (Reizis *et al.*, 1997) are double homozygous for the SCID mutation (Ueda *et al.*, 2000) and carry the IL-2 receptor γ allelic mutation (γ_c^{null}) (Mamoru *et al.*, 2002). For this reason, there is no immediate indication of how the parallel downregulation of GFAP and MHC II might be mediated. The reduction in macrophage function apparent in these mice probably contributes to lowering MHC II staining in the dermis, but our results suggest that there may be an additional coordinated response in GFAP-PCs. The possibility is that this is a consequence of the IL-2 receptor γ null mutation that needs to be addressed in further studies.

A comparison of the properties of GFAP-PCs in the integumentary system and in inner organs lends further support to a functional association between GFAP and MHC II. In skin, the absence of MHC II has been noted in diseases that affect pigmentation (Marks *et al.*, 2003). In this respect, it is interesting that both MHC II and GFAP are expressed at very low levels in melanoma sections, that is, under conditions requiring avoidance of immune surveillance (article in preparation). In inner organs, coexpression of GFAP and MHC II is apparent in healthy spleen antigen-presenting cells; non-differentiated HSCs (Buniatian, 2001, 2003b, unpublished results; Riccalton-Banks *et al.*, 2003; Vinas *et al.*, 2003); healthy kidney glomerular mesangial cells, and podocytes (Pfaff *et al.*, 1999) – all cells located adjacent to fenestrated capillaries. Furthermore, the parallel upregulation of GFAP and MHC II has been described in astrocytes during pathologic situations involving disturbance of the blood–brain barrier (Ransohoff and Estes, 1991;

Zeinstra *et al*., 2000), which are further characterized by the acquisition of antigen-presenting capacity by microglia and invasion of T lymphocytes specific for neural antigens within the central nervous system (Lassmann *et al*., 1994; Neumann, 2001). Thus, GFAP might be an indicator of specific local antigen-presenting functions in the skin and other organs.

Skin cells show a general colocalization of MT with GFAP, although the MT/GFAP ratio may vary and appears to be highest in the basal layer and in distinct structures such as the papilla. The mAb against MT used in this study specifically reacts with Cd/Zn-MT-I – a molecular species of MT which is not found in quiescent HSC, but is expressed upon activation (Buniatian *et al*., 2001; Lu *et al*., 2001). The same is true for functionally active astrocytes and for activated podocytes and mesangial cells (for review, see Chin and Templeton, 1993; Buniatian *et al*., 2001, 2002). Thus, colocalization of GFAP and MT in certain skin cells at the air–tissue interface is indicative of an activated phenotype. In this respect, it is noteworthy that the MT gene is upregulated in skin following topical application of zinc and copper, and in wound margins, particularly in regions of high mitotic activity (for review, see Lansdown, 2002).

In conclusion, the skin shows a high proportion of GFAP-PC, supporting the view that cells of this phenotype play an important role in forming a permselective barrier not only at blood–tissue interfaces in internal organs (Buniatian, 2001, 2003a, b), but also at the air–body interface in the integumentary system. The coordinated expression of specific molecules involved in protection and proliferation (MT, MHC II) further emphasizes the important role of the skin in the defense of the whole organism against environmental insults.

MATERIALS AND METHODS

Antibodies

mAb against GFAP, clone GF 12.24 (dilution 1:10, Progen Biotechnik GmbH, Heidelberg, Germany); pAb against bovine GFAP (dilution 1:250 Dako, Glostrup, Denmark); Mouse mAb against porcine vimentin, clone 9 (dilution 1:40 Sigma, Deisenhofen, Germany); Mouse mAb against porcine desmin, clone DE-U10 (dilution 1:33, Amersham-Buchler Braunschweig, Germany); Mouse mAb against SMAA, derived from clone ASM-1 (dilution 1:100 Progen, Heidelberg, Germany); Mouse mAb against MHC II (dilution 1:100, Harlan Sera-Lab Limited (Loughborough, UK); Mouse mAb against Cd/Zn-MT (1.7 μg/μl, dilution 1:100) was generous gift of Dr U. Weser, Institute of Biochemistry of University of Tübingen, Germany (Nagel *et al*., 1990; Buniatian *et al*., 2001); FITC-labelled goat anti-rabbit IgG (dilution 1:100), Cy3-conjugated goat anti-mouse IgG (dilution 1:800) and Horseradish Peroxidase HRP-goat anti-mouse IgG conjugate (dilution 1:1000 Dianova GmbH, Hamburg, Germany).

Animals

All rats and mice were maintained at the central animal facility according to Institutional Guidelines for Ethical Care of Animals. C57BL/6 and CD1 BalbC mice were bred at the same animal facility and used as skin donors after 1–2 weeks of age. NOD/SCID/γ_c^{null} and CD1-Foxn1 nu mice were originally bought from Charles River (Sulzfeld, Germany) as were newborn Sprague–Dawley rats (250–300 g).

Human skin

The experiments were performed using operative material obtained from the Childrens Hospital or the dermatological department of the University of Leipzig. Samples of human foreskin and adult skin from healthy skin regions adjacent to operated areas, were obtained with consent from patients in accordance with the Declaration of Helsinki Principles and under the license of the Ethic Commission of the Leipzig University. Cell cultures were established from postoperative tissues taken from healthy areas of foreskins. The foreskins from 2- to 8-year-old children were placed in sterile phosphate-buffered saline (PBS) immediately after operation stored at 4°C until use.

Rodent skin

Samples of rat skin were prepared from the scalp of newborn rats after extirpation of the brain which was used for the preparation of astroglial primary cultures. Likewise, samples from mouse skin were extirpated from the same area of mice used for the preparation of hepatocytes. Skin material was freed from fat and frozen immediately at 80°C.

Cell culture

Keratinocytes. Primary normal human epidermal keratinocytes were isolated from the foreskins of 2- to 8-year-old children as described previously (Zellmer and Reissig, 2001), seeded in Petri dishes containing coverslips. The cells were grown in serum-free keratinocyte growth medium (Clonetics, San Diego, CA) containing 0.15 mM $CaCl_2$, 0.1 μg/ml human epidermal growth factor (Clonetics), 0.5 μg/ml hydrocortisone, 5 μg/ml insulin, 30 μg/ml bovine pituitary extract, 50 μg/ml gentamycin, and 50 μg/ml amphotericin. Cultures were terminated at day 7 by brief washing in PBS, followed by fixation in ice-cold methanol at −20°C for 10 minutes.

Fibroblasts. Monolayers of normal human dermal fibroblasts from the foreskins of 2- to 8-year-old children were obtained from explants culture of de-epidermized skin and cultured in DMEM containing 10% heat-inactivated fetal calf serum (Gibco, Grand Island, NY), 50 μg/ml L-ascorbic acid, 100 U/ml penicillin, and 100 μg/ml streptomycin sulfate, as described previously (Bayreuther *et al*., 1992). The fibroblast cultures were kept in an incubator with 5% CO_2 in air (95% humidity) at 37°C. Cultures were terminated at day 1 and 3 in culture as described above.

T6 cells. The GFAP-containing T6 cells, an activated HSC cell line (Kim *et al*., 1998) was a generous gift of Dr Scott Friedman (Division of Liver Diseases, Mount Sinai School of Medicine, New York). T6 cells from 5 to 10 passages were cultured in DMEM containing 10% fetal calf serum, 20 U/ml penicillin 20 μg/ml streptomycin sulfate.

Astrocytes. Astroglia-rich primary cultures were prepared from brains of newborn rats as described elsewhere (Hamprecht and Löffler, 1985).

Immunohistochemistry and immunocytochemistry

The foreskins from 2- to 8-year-old children, adult human skin, rat, and mouse scalps were separated from fat tissue, washed twice with

sterile PBS at 4°C, and frozen in liquid nitrogen. Unfixed 7 μm cryostat sections of human and rat skin were prepared as described previously (Buniatian *et al*., 1996b). After fixation in methanol (−20°C), the cells and tissue slices were washed with PBS at room temperature. In monolabelling studies, the cells were exposed to pAb anti-GFAP antiserum, or to mouse mAbs against GFAP, or against SMAA, or against MHC II. Double-immunolabelling studies were performed using mixtures of pAb anti-GFAP with mAbs against either MT, or desmin, or vimentin, or SMAA, or MHC II. The mAb MT used in this study specifically reacted with Cd/Zn-MT-I produced by SMAA-positive astrocytes, HSCs, podocytes, and mast cells (Buniatian *et al*., 2001, 2002). After 2 hour incubation at room temperature, specimens were washed and exposed for 1 hour at room temperature to a mixture of the secondary antibodies: FITC-conjugated anti-rabbit IgG and Cy3-conjugated anti-mouse IgG. All antibodies were diluted with PBS in concentrations indicated above. After washing the cells with PBS containing Triton X-100 (Sigma, Deisenhofen, Germany), the cells and tissues were mounted in Vectashield mounting medium containing DAPI (Vector Laboratories, Burlingame, CA) and examined with a fluorescence microscope B × 51 (Olympus Optical Co. Europe, Hamburg, Germany) with UplanFl 20 ×/0.5 Ph1; UPlanFl 10 ×/0.30 Ph1; UPlanFl 40 ×/0.75 Ph2 objectives. Images were taken with the digital camera F-View II (Soft Imaging System, Leinfelden-Echterdingen, Germany) at room temperature and data were processed with AnalysisDOKU® (Imaging System GmbH, Leinfelden-Echterdingen, Germany). The rat and mouse skin was fixed in ice-cold methanol without preliminary treatment.

CLS microscopy

CLS microscopy was performed on a Leica SL CLS microscope equipped with an argon/krypton laser (Leica Lasertechnik, Heidelberg, Germany). To improve the signal-to-noise ratio, eight scans of one focal plane were averaged. The confocal image data were obtained using a PLANAPO 63 ×, 1.32 NA oil immersion objective and CLS microscope software (Leica Lasertechnik), and processed with Adobe Photoshop 7.0 software (Adobe Systems Inc., Mountain View, CA).

Immunoblotting

Separation of the proteins from newborn rat skin and brain homogenates and T6 cell line and newborn rat astroglial culture homogenates was performed in SDS-PAGE according to Laemmli, (1970) and the proteins were electroblotted onto a nitrocellulose membrane (Burnette, 1981). Briefly, SDS-PAGE was conducted using 10% (w/v) acrylamide gels. The proteins were electroblotted onto a nitrocellulose membrane at a current of 0.3 A for 12 hours in transfer buffer (25 mM Tris, 192 mM glycine, pH 9.0). The membrane was blocked using 5% (w/v) milk powder in incubation buffer (20 mM Tris-HCl, 150 mM NaCl, 0.02% (w/v) Tween-20, pH 7.4) at room temperature for 1 hour. The filters were washed four times with incubation buffer and incubated with mAb GFAP (dilution 1:1000; Progen Biotechnik GmbH, Heidelberg, Germany) overnight. Subsequently, the membrane was incubated with horseradish-peroxidase-conjugated anti-mouse IgG (secondary antibody) at a dilution of 1:1000 for 3–5 minutes. The membrane was washed four times with incubation buffer and immunocomplexes were visualized using luminol-based enhanced chemiluminescence Western blotting reagent (ECLR, Amersham Biosciences, Freiburg, Germany).

CONFLICT OF INTEREST

The authors state no conflict of interest.

ACKNOWLEDGMENTS

We thank Doris Mahn, Frank Struck, and Ulrike Ties for excellent technical assistance and Dr Michael Cross for critical reading of the discussion.

REFERENCES

Apte MV, Haber PS, Applegate TL, Norton ID, McCaughan GW, Korsten MA *et al*. (1998) Periacinar stellate shaped cells in rat pancreas: identification, isolation, culture. *Gut* 43:128–33

Bayreuther K, Francz PI, Gogol J, Kontermann K (1992) Terminal differentiation, aging, apoptosis, spontaneous transformation in fibroblast stem cell systems *in vivo in vitro*. *Ann NY Acad Sci* 663:167–79

Brenner M (1994) Structure and transcriptional regulation of the GFAP gene. *Brain Pathol* 4:245–57

Buniatian G, Gebhardt R, Schrenk D, Hamprecht B (1996a) Co-localisation of three types of intermediate filament proteins in perisinusoidal stellate cells: glial fibrillary acidic protein as a new cellular marker. *Eur J Cell Biol* 70:23–32

Buniatian G, Hamprecht B, Gebhardt R (1996b) Glial fibrillary acidic protein as a marker of perisinusoidal stellate cells that can distinguish between the normal and myofibroblast-like phenotypes. *Biol Cell* 87: 65–73

Buniatian GH (2001) Similar protective features of activated hepatic stellate cells and healthy astrocytes. In: *Cells of hepatic sinusoid* (Wisse E, Knook DL, de Zanger R, Fraser R, eds), vol 8. Netherls: The Kupffer Cell Foundation, 200–4

Buniatian GH (2003a) Stages of activation of hepatic stellate cells (HSC): effects of ellagic acid, an inhibiter of liver fibrosis, on the antigenic morphologic differentiation of cultured HSC. *Cell Prolif* 38:307–19

Buniatian GH (2003b) Common features of perivascular cells of the spleen and liver. *Eur J Cell Biol* 102(Suppl):4–8. Abstract

Buniatian GH, Gebhardt R, Mecke D, Traub P, Wiesinger H (1999a) Common myofibroblastic features of newborn rat astrocytes cirrhotic rat liver stellate cells in early cultures *in vivo*. *Neurochem Int* 35:317–27

Buniatian GH, Gebhardt R, Traub P, Mecke D, Osswald H (1999b) Dynamics of the distribution of glial fibrillary acidic protein in cultured myofibroblast-like cells of rat kidney: glomerular podocytes mesangial cells. *Biol Cell* 91:675–84

Buniatian GH, Hartmann H-J, Traub P, Weser U, Wiesinger H, Gebhardt R (2001) Acquisition of blood–tissue barrier supporting features by hepatic stellate cells astrocytes of myofibroblastic phenotype. Inverse dynamics of metallothionein glial fibrillary acidic protein expression. *Neurochem Int* 38:373–83

Buniatian GH, Hartmann H-J, Traub P, Wiesinger H, Albinus M, Nagel W *et al*. (2002) Glial fibrillary acidic protein-positive cells of the kidney are capable of raising a protective biochemical barrier similar to astrocytes: expression of metallothionein in podocytes. *Anat Rec* 267:296–306

Bunn RC, Jensen MA, Reed BC (1999) Protein interactions with the glucose transporter binding protein GLUT1CBP that provide a link between GLUT1 and the cytoskeleton. *Mol Biol Cell* 10:819–32

Burnette WN (1981) ''Western blotting'': electrophoretic transfer of proteins from sodium dodecyl sulphate-gels to unmodified nitrocellulose radiographic detection with antibody radioiodinated protein A. *Anal Biochem* 112:195–203

Cassiman D, van Pelt J, De Vos R, Van Lommel F, Desmet V, Yap SH *et al*. (1999) Synaptophysin: a novel marker for human rat hepatic stellate cells. *Am J Pathol* 155:1831–9

Chin TA, Templeton DM (1993) Protective elevations of glutathione and metallothionein in cadmium-exposed mesangial cells. *Toxicology* 77:145–56

Condorelli DF, Nicoletti VG, Barresi V, Conticello SG, Caruso A, Tendi EA *et al*. (1999) Structural features of the rat GFAP gene identification of a novel alternative transcript. *J Neurosci Res* 56:219–28

Dupasquier M, Stoitzner P, van Oudenaren A, Romani N, Leenen PJ (2004) Macrophages and dendritic cells constitute a major subpopulation of cells in the mouse dermis. *J Invest Dermatol* 123:876–9

Duraiswamy N, Tse Y, Hammerberg C, Kang S, Cooper KD (1994) Distinction of class II MHC+ Langerhans cell-like interstitial dendritic antigen-presenting cells in murine dermis from dermal macrophages. *J Invest Dermatol* 103:678–83

Gaspari AA (1997) The role of keratinocytes in the pathophysiology of contact dermatitis. *Immunol Allergy Clin North Am* 17:377–405

Gaspari AA, Katz SI (1988) Induction and functional characterization of Class II MHC (Ia) antigens on murine keratinocytes. *J Immunol* 140:2956–63

Gilhar A, Kalish RS (2006) Alopecia areata: a tissue specific autoimmune disease of the hair follicle. *Autoimmun Rev* 5:64–9

Hainfellner JA, Voigtländer T, Ströbel T, Mazal PR, Maddalena AS, Aguzzi A *et al.* (2001) Fibroblast can express glial fibrillary acidic protein (GFAP) *in vivo*. *J Neuropath Exp Neurol* 60:449–61

Hamprecht B, Löffler F (1985) Primary glial cultures as a model for studying hormonal action. *Methods Enzymol* 109:341–5

Holash JA, Harik SI, Perry G, Stewart PA (1993) Barrier properties of testis microvessels. *Proc Natl Acad Sci USA* 90:11069–73

Kim Y, Ratziu V, Choi SG, Lalazar A, Theiss G, Dang Q *et al.* (1998) Transcriptional activation of transforming growth factor beta1 its receptors by the Kruppel-like factor Zf9/core promoter-binding protein Sp1. Potential mechanisms for autocrine fibrogenesis in response to injury. *J Biol Chem* 273:33750–8

Laemmli UK (1970) Cleavage of structural proteins during the assembly of the head of bacteriophage T_4. *Nature* 227:680–5

Lansdown AB (2002) Metallothioneins: potential therapeutic aids for wound healing in the skin. *Wound Repair Regen* 10:130–2

Lassmann H, Suchanek G, Ozawa K (1994) Histopathology and the blood–cerebrospinal fluid barrier in multiple sclerosis. *Ann Neurol* 36:S42–6

Lecain E, Alliot F, Laine MC, Calas B, Pessac B (1991) Alpha isoform of smooth muscle actin is expressed in astrocytes *in vitro in vivo*. *J Neurosci Res* 28:601–6

Lonigro R, Donnini D, Zappia E, Damante G, Bianchi ME, Guazzi S (2001) Nestin is a neuroepithelial target gene of thyroid transcription factor-1, a homeoprotein required for forebrain organogenesis. *J Biol Chem* 276:47807–13

Lu SC, Alvarez L, Huang ZZ, Chen L, An W, Corrales F *et al.* (2001) Methionine adenosyltransferase 1A knockout mice are predisposed to liver injury exhibit increased expression of genes involved in proliferation. *Proc Natl Acad Sci USA* 98:5560–5

Mamoru I, Hiramatsu H, Kobayashi K, Suzue K, Kawahata M, Hioki K *et al.* (2002) NOD/SCID/γ_c^{null} mouse: an excellent recipient mouse model for engraftment of human cells. *Blood* 100:3175–82

Mani N, Khaibullina A, Krum JM, Rosenstein JM (2005) Astrocyte growth effects of vascular endothelial growth factor (VEGF) application to perinatal neocortical explants: receptor mediation signal transduction pathways. *Exp Neurol* 192:394–406

Marks MS, Theos AC, Raposo G (2003) Melanosomes and MHC class II antigen-processing compartments: a tinted view of intracellular trafficking and immunity. *Immunol Res* 27:409–26

Mecklenburg L, Tychsen B, Paus R (2005) Learning from nudity: lessons from the nude phenotype. *Exp Dermatol* 14:797–810

Nagel W, Hartmann H-J, Weser U (1990) Monoclonal antibodies to monomeric rat liver metallothionein-I: the immunoreactivity of lysine residues in metallothionein. *Immunol Lett* 26:291–9

Neumann H (2001) Control of glial immune function by neurons. *Glia* 36:291–5

Niki T, De Bleser PJ, Xu G, Van Den Berg K, Wisse E, Geerts A (1996) Comparison of glial fibrillary acidic protein desmin staining in normal CCl_4-induced fibrotic rat livers. *Hepatology* 23:1538–45

Oren A, Ganz T, Liu L, Meerloo T (2003) In human epidermis, beta-defensin 2 is packaged in lamellar bodies. *Exp Mol Pathol* 74:180–2

Peterson LJ, Rajfur Z, Maddox AS, Freel CD, Chen Y, Edlund M *et al.* (2004) Simultaneous stretching contraction of stress fibers *in vivo*. *Mol Biol Cell* 15:3497–508

Pfaff IL, Wagner HJ, Vallon V (1999) Immunolocalisation of protein kinase C isoenzymes alpha, beta1 betaII in rat kidney. *J Am Soc Nephrol* 10:1861–73

Ransohoff RM, Estes ML (1991) Astrocyte expression of major histocompatibility complex gene products in multiple sclerosis brain tissue obtained by stereotactic biopsy. *Arch Neurol* 48:1244–6

Reizis B, Eisenstein M, Bockoba J, Könen-Waisman S, Mor F, Elias D *et al.* (1997) Molecular characterization of the diabetes-associated mouse MHC class II protein, I-A^{87}. *Int Immunol* 9:43–51

Riccalton-Banks L, Bhari R, Fry J, Shakesheff KM (2003) A simple method for the simultaneous isolation of stellate cells hepatocytes from rat liver tissue. *Mol Cell Biochem* 248:97–102

Schulze W, Davidoff MS, Holstein AF (1987) Are Leydig cells of neural origin? Substance P-like immunoreactivity in human testicular tissue. *Acta Endocrinol (Copenhagen)* 115:373–7

Schwab JM, Beschorner R, Nguyen TD, Meyermann R, Schluesener HJ (2001) Differential cellular accumulation of connective tissue growth factor defines a subset of reactive astrocytes, invading fibroblasts, endothelial cells following central nervous system injury in rats humans. *J Neurotrauma* 18:377–88

Steinert PM, Chou YH, Prahlad V, Parry DA, Marekov LN, Wu KC *et al.* (1999) A high molecular weight intermediate filament-associated protein in BHK-21 cells is nestin, a type VI intermediate filament protein. Limited co-assembly *in vitro* to form heteropolymers with type III vimentin type IV alpha-internexin. *J Biol Chem* 274:9881–90

Tolstonog GV, Wang X, Shoeman R, Traub P (2000) Intermediate filaments reconstituted from vimentin, desmin, glial fibrillary acidic protein selectively bind repetitive mobile DNA sequences from a mixture of mouse genomic DNA fragments. *DNA Cell Biol* 19: 647–77

Traub P (1995) Intermediate filaments gene regulation. *Physiol Chem Phys Med NMR* 27:377–400

Ueda T, Yoshino H, Kobayashi K, Kawahata M, Ebihara Y, Ito M *et al.* (2000) Hematopoietic repopulating ability of cord blood CD34(+) cells in NOD/Shi-scid mice. *Stem Cells* 18:204–13

Vinas O, Bataller R, Sancho-Bru P, Gines P, Berenguer C, Enrich C *et al.* (2003) Human hepatic stellate cells show features of antigen-presenting cells stimulate lymphocyte proliferation. *Hepatology* 38: 919–29

Wagner AP, Reck G, Platt D (1993) Evidence that V^+ fibronectin, GFAP S100 beta RNAs are increased in the hyppocampus of aged rats. *Exp Gerontol* 28:135–43

Zeinstra E, Wilczak N, Streefland C, De Keyser J (2000) Astrocytes in chronic active multiple sclerosis plaques express MHC class II molecules. *Neuroreport* 11:89–91

Zellmer S, Reissig D (2001) Isolation, cultivation differentiation of normal human keratinocytes in serum-free medium. In: *Epithelial cell culture protocols* (Wise C, ed), Totowa, New Jersey: Humana Press Inc., 179–84